Appendix

Content:

A

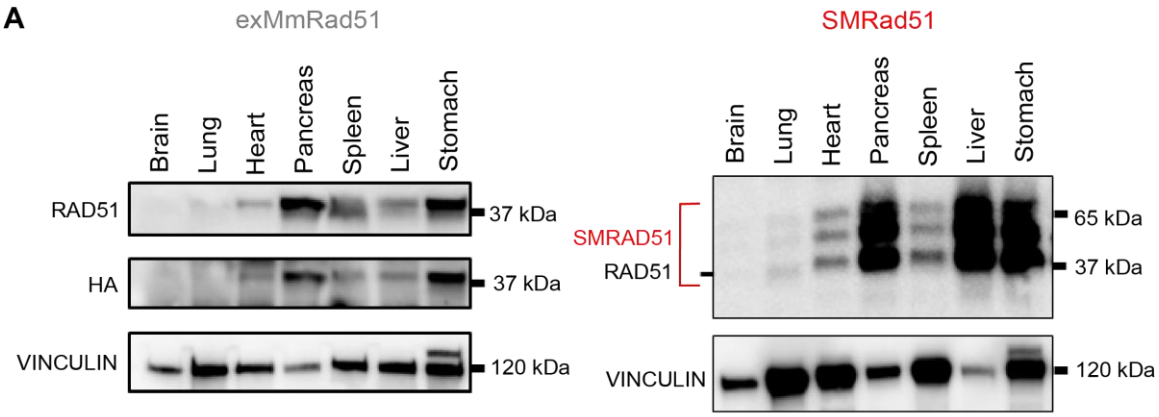

B

Organ	Phenotype	SMRAD51 expression
Pancreas	Normal histology	Yes
Heart	Normal histology	Yes
Lung	Normal histology	Yes
Liver	Normal histology	Yes
Spleen	Normal histology	Yes
Small intestine	Normal histology	Yes
Testis	Features of arrested development	Yes
Skin	Few and abnormal hair folicules, acanthosis, numerous inflammatory cells	Yes

C

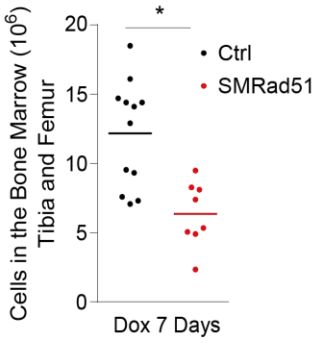

Appendix Figure S1. Histopathological analysis of young growing mice after expression of *SMRad51* for 12 days. (A) Western blot analysis of exMmRAD51 and SMRAD51 protein content in extracts from various tissues of young mice after 5 days of Dox treatment. **(B)** Summary of the results of pathological analysis and SMRAD51 presence assessment by immunohistochemistry in various tissues of SMRad51 and Ctrl mice. At least 3 different mice of each genotype were analyzed. **(C)** Cell numbers in tibia and femur bone marrow samples from young Ctrl and SMRad51 mice after 7 days of Dox

treatment. Each point represents a biological replicate and the horizontal bar show the mean. Statistical analysis: Student's t-test. *$p<0.05$.

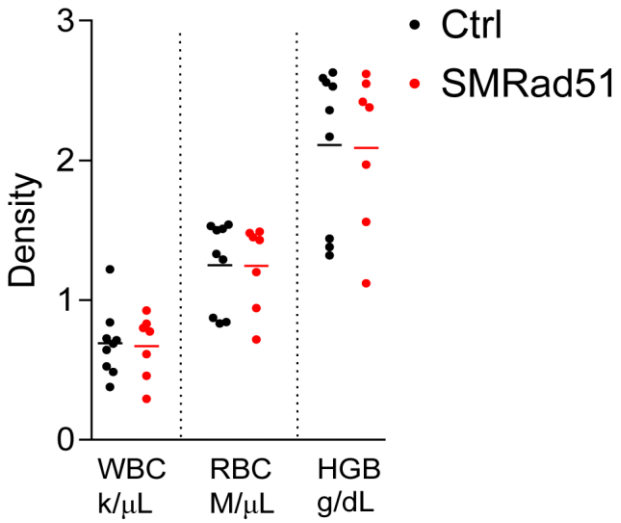

Appendix Figure S2. *SMRad51* expression for 7 days does not change basic blood parameters. WBC, RBC and HGB density analysis of blood samples from growing mice after 7 days of Dox treatment in Ctrl (n=9) and SMRad51 (n=7) mice. Each point represents a biological replicate and the horizontal bar show the mean.

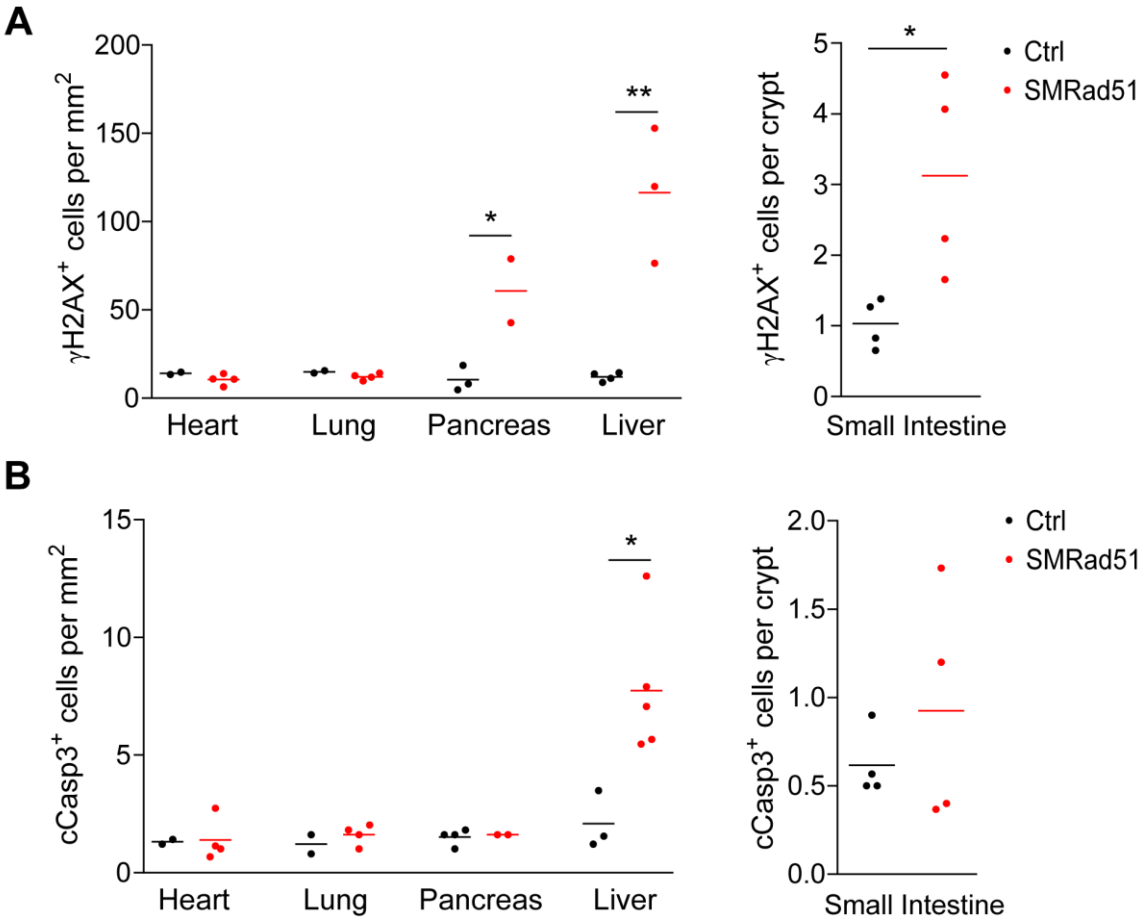

Appendix Figure S3. *SMRad51* expression in growing mice leads to tissue-specific DDR activation and apoptosis. **A.** Quantification of γH2AX⁺ cells in various tissues of Ctrl and SMRad51 mice after 12 days of Dox treatment. **B.** Quantification of cCasp3⁺ positive cells in various tissues of Ctrl and SMRad51 mice after 12 days of Dox treatment. Each point represents a biological replicate and the horizontal bar show the mean. Statistical analysis: Student's t-test. * $p<0.05$; ** $p<0.01$.

Appendix Table S1. Pre-mature ageing phenotypes compared to other models of DNA repair and/or progeroid syndrome

Phenotype	*ERCC1*$^{-/-}$ (Weeda *et al*, 1997; Robinson *et al*, 2018; Dollé *et al*, 2011)	*XPD*^{TTD} (De Boer *et al*, 2002; Wijnhoven *et al*, 2005)	*mTR*$^{-/-}$ (Rudolph *et al*, 1999)	*ATR*$^{s/s}$ (Murga *et al*, 2009; Ruzankina et al. 2007)	*BRCA1*$^{\Delta 11}$*53BP1*^{S25A} (Callen *et al*, 2020)	SMRad51	ExMmRad51	*Lmna*$^{HG/+}$ (Yang *et al*, 2008)
Hair Loss	-	+	+	+	na	+	-	na
Kyphosis	+	+	+	+	+	+	-	+
Reduced Activity	+	na	na	na	+	+	-	na
Priapism	+	na	na	na	na	+	-	na
Decreased Body weight	+	+	+	+	+	+	-	+
Subcutaneous Fat Loss	+	+	+	na	na	+	-	+

n/a = not available

Appendix Table S2. Classification of Cytokines and Chemokines presented in Figure 2 (Turner et al. 2014 http://dx.doi.org/10.1016/j.bbamcr.2014.05.014)

CYTOKINES	**pro-inflammatory cytokines**	**anti-inflammatory cytokines**	**adaptive immunity cytokines**
	IL-1a Il-1b IL-1ra INF-g	IL-23 IL-27 IL-28	IL-3 IL-5 IL-2 IL-15 IL-13
CHEMOKINES	**angiostatic chemokines**	**allergic pro-inflammatory chemokines**	**matrix remodeling**
	CXCL11	CCL17	MMP-3 MMP-9

CXCL16= pro-inflammatory chemokine induced by IFNg

CCL12= chemo-attracted chemokine (monocytes, eosinophils)
CCL20 or MIP3A (Macrophage Inflammatory Protein-3)= pro-inflammatory chemokine

CXCL13= chemo-attracted chemokine (lymphocytes B)

Appendix Table S3. List of primers used for real time RT-PCR.

Gene Symbol	Forward primer 5' - 3'	Reverse primer 5' - 3'
β-Actin	GCCCTGAGGCTCTTTTCCAG	TGCCACAGGATTCCATACCC
Gapdh	AGGTCGGTGTGAACGGATTG	TGTAGACCATGTAGTTGAGGTCA
Il6	TAGTCCTTCCTACCCCAATTTCC	TTGGTCCTTAGCCACTCCTTC
Ccl2	TTAAAAACCTGGATCGGAACCAA	GCATTAGCTTCAGATTTACGGGT
IIIβ	CAGGCAGGCAGTATCACTCA	AGCTCATATGGGTCCGACAG
Tnfα	GAACTGGCAGAAGAGGCACT	AGGGTCTGGGCCATAGAACT
Cxcl1	CTGGGATTCACCTCAAGAACATC	CAGGGTCAAGGCAAGCCTC

Appendix material and methods

Colony formation assay

For a colony formation assay, one hundred exMmRad51 or SMRad51 iMEFs were plated per well in 6-well plates. After 24 h, the cells were treated or not treated with 10 µg/mL doxycycline, and 24 h later, the cells were treated or not with mitomycin C (MMC; Roche #10107409001) or olaparib (Selleckchem #S1060) for 10 days. The drugs were added only once at the start of the treatment. The clones were stained with crystal violet and counted.

Homology-dependent gene targeting assay

The gene targeting procedure was derived from (Zhang *et al*, 2014). This protocol consists of replacing the second exon of the 53BP1 gene with a hygromycin resistance (Hyg^+) gene using a homology-dependent donor plasmid (here called pDonor) after Cas9-mediated production of a DNA DSB. A total of 300,000 cells were resuspended in 100 µL of nucleofection buffer (Lonza #VCA-1003) containing 1 µg of pCas9 and 2 µg of pDonor with or without 1 µg of pgRNA1 or pgRNA2. The cells were nucleofected using Amaxa (Lonza) protocol T30. Immediately after nucleofection, 500 µL of medium was added, and the cells were plated on a 10 mm petri dish. After 48 h, the targeted clones (Hyg^+) were selected for 10 days with medium containing hygromycin that was renewed every 48 h. The clones were stained with crystal violet and counted.

Protein purification

Previously generated pcDNA3.1-MmRad51 and pcDNA3.1-SMRad51 constructs (Lambert & Lopez, 2000) encoding sequences were subcloned into a pCDF-His-SUMO backbone using a complementary single-strand annealing-based method. His-SUMO-MmRAD51 and his-SUMO-SMRAD51 were both expressed in the *E. coli* strain BRL(DE3)pLysS. All of the protein purification steps were carried out at 4°C. Protein expression was induced in 3 L of cell culture medium with 0.5 mM isopropyl-1-thio-β-D-galactopyranoside overnight at 20°C, after which the cells were resuspended in PBS with 350 mM NaCl, 20 mM imidazole, 10% glycerol, 0.5 mg/mL lysozyme, complete protease inhibitor (Roche), and 1 mM 4-(2-aminoethyl)benzenesulfonyl fluoride (AEBSF). Then, the cells were lysed by sonication, and the insoluble material was removed by centrifugation at 150,000 × *g* for 1 h. The supernatant was incubated with 5 mL of Ni-NTA resin (Qiagen) for 2 h. The mixture was poured into an Econo-Column Chromatography Column (Bio-Rad), and the beads were washed with 80 mL of W1 buffer (20 mM Tris HCl pH 8, 500 mM NaCl, 20 mM imidazole, 10% glycerol, 0.5% NP40) followed by 80 mL of W2 buffer (20 mM Tris HCl pH 8, 100 mM NaCl, 20 mM imidazole, 10% glycerol, 1 mM DTT). His-SUMO-tagged proteins bound to the beads were then resuspended in 8 mL of W2 buffer and incubated with SUMO protease at a ratio of 1/80 (w/w) for 16 h. The proteins in which the His-SUMO tag was cleaved were then recovered in the flowthrough and directly loaded onto a HiTrap heparin column (GE Healthcare). The column was washed with W2 buffer, and then a 0.1-1 M NaCl gradient was applied. Fractions containing purified proteins were dialyzed against storage buffer (20 mM Tris HCl pH 8, 50 mM KCl, 0.5 mM EDTA, 10% glycerol, 1 mM DTT, 0.5 mM AEBSF), aliquoted and stored at -80°C. The concentrations of purified MmRad51 and SMRad51 were calculated using extinction coefficients of 1.664×10^4 $M^{-1}cm^{-1}$ and 1.813×10^4 $M^{-1}cm^{-1}$ at 280 nm, respectively.

D-Loop assay

For the D-loop assay, 19 nM molecules (7.5 µM nt) of a 400 nulcetides ssDNA labeled with the Cy5 fluorophore were incubated with MmRAD51, SMRAD51 or both (SM:MmRAD51 ratio: 0, 8, 16, 24, 32, 48 and 100%) at a final concentration of 25 µM (1 protein per 3 nt) for 3 minutes at 37°C. RPA was then added to a final concentration of 0.075 µM (1 protein per 100 nt) over a span of 15 minutes in buffer containing 10 mM Tris-HCl (pH 8), 50 mM sodium chloride, 2 mM calcium chloride, 2 mM Magnesium

chloride, 1 mM DTT and 1.5 mM ATP. Then, a homologous double-stranded DNA (dsDNA) pUC19 plasmid (purchased from New England Biolabs) was added to the reaction at a concentration of 16 nM molecules in a final volume of 8 µL over a span of 30 minutes. The total reaction was stopped by the addition of 1% SDS (w/v) plus 25 mM EDTA and deproteinized (by 30 minutes of incubation at 37°C with 2 mg/mL proteinase K). The samples were run in a 1.2 % (w/v) agarose gel at 80 V for 35 minutes in 0.5× TAE buffer. Fluorolabeled DNA species were visualized by using a Typhoon FLA 9500 (GE Healthcare Life Sciences).

TEM analysis of RAD51 filaments

RAD51 presynaptic filaments were assembled on a 5' DNA junction with a single-stranded overhang (the construction of which has been described in (Tavares *et al*, 2019) using MmRAD51, SMRAD51 or a mix of both, as follows: 0.2 µM (36 µM nt) of 5' junction DNA molecules were incubated with MmRAD51, SMRAD51 or both at a final concentration of 12 µM (1 protein per 3 nt) for 5 minutes at 37°C. RPA was then added to a final concentration of 0.6 µM (1 protein per 100 nt) over a span of 10 minutes in buffer containing 10 mM Tris-HCl (pH 8), 50 mM sodium chloride, 2 mM calcium chloride, 1 mM DTT and 1.5 mM ATP. The reactions were quickly diluted 25× in buffer, and a 5 µL drop was deposited on a 600-mesh copper grid previously covered with a thin carbon film and activated with pentylamine by glow discharge using a Dubochet device. Each grid was rinsed, positively stained with aqueous 2% (w/v) uranyl acetate, dried carefully with filter paper and observed in annular dark-field mode using a Zeiss 902 transmission electron microscope. Images were captured at a magnification of 85,000× with a MegaViewIII charge-coupled device (CCD) camera and analyzed with iTEM software (Olympus Soft Imaging Solution).

Western blotting.

Cells were lysed in buffer containing 20 mM Tris HCl (pH 7.5), 1 mM Na_2EDTA, 1 mM EGTA, 150 mM NaCl, 1% (w/v), 1 mM β-glycerophosphate, NP40, 1% sodium deoxycholate, 2.5 sodium pyrophosphate, 1 mM NA_3VO_4, 1 µg/ml leupeptin and complete ULTRA Tablets (Roche, Basel, Switzerland). Denatured proteins (20-40 µg) were electrophoresed in 9% SDS-PAGE gels or MiniPROTEAN® TGX™ 4-15% Precast gels (Bio-Rad, Hercules, CA, USA) transferred onto a nitrocellulose membrane and probed with specific antibodies. Anti-Vinculin (1/8,000, SPM227, ab18058, Abcam, Cambridge, UK), anti-RAD51 (1/1,000, Ab-1, PC130, Millipore, Burlington, MS, USA). Immunoreactivity was visualized through an enhanced chemiluminescence detection kit (ECL, Pierce).

Measurement of SSA and EJ efficiency by FACS.

Cells were transfected with the pCBASceI plasmid (Addgene, Watertown, MA, USA, #26477) and incubated for 72 hours. Then cells were collected with 50 mM EDTA diluted in PBS, pelleted and fixed with 2% paraformaldehyde for 20 minutes. The percentage of GFP-expressing cells was scored by FACS analysis using a BD Accuri C6 flow cytometer (BD, Franklin Lakes, NJ, USA). The percentage of CD4-expressing cells was measured after incubation for 10 minutes with 1 µl of anti-CD4 antibody coupled to Alexa 647 (rat isotype, RM4-5, Invitrogen, Waltham, MA, USA).

Appendix References

Callen E, Zong D, Wu W, Wong N, Stanlie A, Ishikawa M, Pavani R, Dumitrache LC, Byrum AK, Mendez-Dorantes C, Martinez P, Canela A, Maman Y, Day A, Kruhlak MJ, Blasco MA, Stark JM, Mosammaparast N, McKinnon PJ & Nussenzweig A (2020) 53BP1 Enforces Distinct Pre- and Post-resection Blocks on Homologous Recombination. *Mol. Cell* **77:** 26-38.e7

De Boer J, Andressoo JO, De Wit J, Huijmans J, Beems RB, Van Steeg H, Weeda G, Van der Horst GTJ, Van Leeuwen W, Themmen APN, Meradji M & Hoeijmakers JHJ (2002) Premature aging in mice deficient in DNA repair and transcription. *Science (80-.).* **296:** 1276–1279

Dollé MET, Kuiper R V., Roodbergen M, Robinson J, de Vlugt S, Wijnhoven SWP, Beems RB, de la Fonteyne L, de With P, van der Pluijm I, Niedernhofer LJ, Hasty P, Vijg J, Hoeijmakers JHJ & van Steeg H (2011) Broad segmental progeroid changes in short-lived Ercc1 −/Δ7 mice . *Pathobiol. Aging Age-related Dis.* **1:** 7219

Gelot C, Guirouilh-Barbat J, Le Guen T, Dardillac E, Chailleux C, Canitrot Y & Lopez BSBSBS (2016) The Cohesin Complex Prevents the End Joining of Distant DNA Double-Strand Ends. *Mol. Cell* **61:** 15–26

Guirouilh-Barbat J, Huck S, Bertrand P, Pirzio L, Desmaze C, Sabatier L & Lopez BSBS (2004) Impact of the KU80 pathway on NHEJ-induced genome rearrangements in mammalian cells. *Mol. Cell* **14:** 611–623

Guirouilh-Barbat J, Rass E, Plo I, Bertrand P & Lopez BSBS (2007) Defects in XRCC4 and KU80 differentially affect the joining of distal nonhomologous ends. *Proc. Natl. Acad. Sci. U. S. A.* **104:** 20902–20907 Available at: http://www.ncbi.nlm.nih.gov/entrez/query.fcgi?cmd=Retrieve&db=PubMed&dopt=Citation&list_uids=18093953

Gunn A & Stark JM (2012) I-SceI-based assays to examine distinct repair outcomes of mammalian chromosomal double strand breaks. *Methods Mol. Biol.* **920:** 379–391

Lambert S & Lopez BS (2000) Characterization of mammalian RAD51 double strand break repair using non lethal dominant negative forms. *EMBO J.* **19:** 3090–3099

Lambert S & Lopez BS (2001) Role of RAD51 in sister-chromatid exchanges in mammalian cells. *Oncogene* **20:** 6627-6631.

Murga M, Bunting S, Montãa MF, Soria R, Mulero F, Cãamero M, Lee Y, McKinnon PJ, Nussenzweig A & Fernandez-Capetillo O (2009) A mouse model of ATR-Seckel shows embryonic replicative stress and accelerated aging. *Nat. Genet.*

Rass E, Grabarz A, Plo I, Gautier J, Bertrand P & Lopez BSBS (2009) Role of Mre11 in chromosomal nonhomologous end joining in mammalian cells. *Nat Struct Mol Biol* **16:** 819–824 Available at: http://www.ncbi.nlm.n

Robinson AR, Yousefzadeh MJ, Rozgaja TA, Wang J, Li X, Tilstra JS, Feldman CH, Gregg SQ, Johnson CH, Skoda EM, Frantz MC, Bell-Temin H, Pope-Varsalona H, Gurkar AU, Nasto LA, Robinson RAS, Fuhrmann-Stroissnigg H, Czerwinska J, McGowan SJ, Cantu-Medellin N, et al (2018) Spontaneous DNA damage to the nuclear genome promotes senescence, redox imbalance and aging. *Redox Biol.* **17:** 259–273

Rudolph KL, Chang S, Lee HW, Blasco M, Gottlieb GJ, Greider C & DePinho RA (1999) Longevity, stress response, and cancer in aging telomerase-deficient mice. *Cell* **96:** 701–712

Ruzankina Y, Pinzon-Guzman C, Asare A, Ong T, Pontano L, Cotsarelis G, Zediak VP, Velez M, Bhandoola A & Brown EJ. (2007) Deletion of the Developmentally Essential Gene ATR in Adult Mice Leads to Age-Related Phenotypes and Stem Cell Loss. Cell Stem Cell **1:** 113-126.

Saintigny Y, Delacote F, Vares G, Petitot F, Lambert S, Averbeck D & Lopez BS (2001)

Characterization of homologous recombination induced by replication inhibition in mammalian cells. *EMBO J* **20:** 3861-3870.

So,A., Dardillac,E., Muhammad,A., Chailleux,C., Sesma-Sanz,L., Ragu,S., Le Cam,E., Canitrot,Y., Masson,J.Y., Dupaigne,P., Lopez,B.S. and Guirouilh-Barbat,J. (2022) RAD51 protects against nonconservative DNA double-strand break repair through a nonenzymatic function. *Nucleic Acids Res* **50:** 2651-2666.

Tavares EM, Wright WD, Heyer WD, Le Cam E & Dupaigne P (2019) In vitro role of Rad54 in Rad51-ssDNA filament-dependent homology search and synaptic complexes formation. *Nat. Commun.* **10:**

Weeda G, Donker I, De Wit J, Morreau H, Janssens R, Vissers CJ, Nigg A, Van Steeg H, Bootsma D & Hoeijmakers JHJ (1997) Disruption of mouse ERCC1 results in a novel repair syndrome with growth failure, nuclear abnormalities and senescence. *Curr. Biol.* **7:** 427–439

Wijnhoven SWP, Beems RB, Roodbergen M, Van Den Berg J, Lohman PHM, Diderich K, Van Der Horst GTJ, Vijg J, Hoeijmakers JHJ & Van Steeg H (2005) Accelerated aging pathology in ad libitum fed XpdTTD mice is accompanied by features suggestive of caloric restriction. *DNA Repair (Amst).* **4:** 1314–1324

Wilhelm T, Magdalou I, Barascu A, Techer H, Debatisse M & Lopez BSBS (2014) Spontaneous slow replication fork progression elicits mitosis alterations in homologous recombination-deficient mammalian cells. *Proc. Natl. Acad. Sci. U. S. A.* **111:** 763–768

Yang SH, Andres DA, Spielmann HP, Young SG & Fong LG (2008) Progerin elicits disease phenotypes of progeria in mice whether or not it is farnesylated. *J. Clin. Invest.* **118:** 3291–3300

Zhang Y, Vanoli F, LaRocque JR, Krawczyk PM & Jasin M (2014) Biallelic targeting of expressed genes in mouse embryonic stem cells using the Cas9 system. *Methods* **69:** 171–178